

ORIGINAL ARTICLE

# Evaluation of epigenetic modulation of cyclooxygenase-2 as a prognostic marker for hepatocellular carcinoma

A Fernández-Alvarez<sup>1,4</sup>, C Llorente-Izquierdo<sup>2,4</sup>, R Mayoral<sup>2,3</sup>, N Agra<sup>2</sup>, L Boscá<sup>2,3</sup>, M Casado<sup>1,3</sup> and P Martín-Sanz<sup>2,3</sup>

Cyclooxygenases (COX-1 and 2) catalyze the first step in prostanoid biosynthesis. They are implicated in homeostatic processes with an important role in inflammation and carcinogenesis. In the liver, COX-2 expression is restricted to proliferation or dedifferentiation situations. The COX-2 promoter contains numerous CpG islands that, when hypermethylated, result in transcriptionally silencing thus regulating the growth of carcinoma cells. In this work, we investigated whether a correlation exists between COX-2 expression and methylation signatures at the 5' region of the gene in hepatoma cell lines and human hepatocellular carcinoma (HCC). We also examined the acetylation status of the COX-2 promoter and the effects of histone deacetylase (HDAC) inhibitors on COX-2 expression. Our results suggest a significant association between reduced COX-2 expression and promoter hypermethylation of COX-2 and histone deacetylation in some hepatoma cell lines and in HCC. Treatment with demethylating agents or HDAC inhibitors restored the expression of COX-2. Moreover, in an HCC cohort, a statistically significant inverse association was observed between COX-2 mRNA levels and promoter methylation. In agreement with these data, a reduction of overall survival of the patients was observed after decreased COX-2 expression by promoter hypermethylation and histone H3 hypoacetylation.

*Oncogenesis* (2012) 1, e23; doi:10.1038/oncsis.2012.23; published online 9 July 2012

**Subject Category:** molecular oncology

**Keywords:** COX-2; promoter methylation; HCC; histone acetylation; survival

## INTRODUCTION

Cyclooxygenases (COX-1 and -2) are the key enzymes in prostanoid biosynthesis. COX-1 is constitutively expressed in many tissues, whereas COX-2 is induced by a variety of stimuli such as growth factors, pro-inflammatory stimuli, hormones and other cellular stresses.<sup>1</sup> Adult hepatocytes fail to induce COX-2 expression regardless of the pro-inflammatory factors used; however, Kupffer, stellate, hepatoma mouse cells and fetal hepatocytes retain the ability to express COX-2 upon stimulation with lipopolysaccharide (LPS) and pro-inflammatory cytokines.<sup>2,3</sup> In this regard, we and others demonstrated that partial hepatectomy (PH) induced COX-2 in hepatocytes and contributed to the progression of cell cycle after PH.<sup>4,5</sup> In addition to liver regeneration after PH or hepatotoxic agents, expression of COX-2 has been detected in animal models of cirrhosis,<sup>6</sup> in human hepatoma cell lines,<sup>7,8</sup> in human hepatocellular carcinoma (HCC)<sup>9</sup> and after hepatitis B or C virus infection.<sup>10,11</sup> Nevertheless, recent data reported that COX-2 mRNA levels were significantly higher in the adjacent liver than in HCC<sup>12</sup> and there was an inverse correlation between COX-2 expression and the differentiation grade and poor prognosis of HCC.<sup>13</sup> Therefore, although the antiapoptotic feature of COX-2 generally supports cancer cell growth, COX-2 downregulation in advanced HCC may be advantageous and specific for HCC development. The mechanisms regulating the expression of COX-2 at specific stages of HCC development remain unknown.

COX-2 is widely regarded as a potential pharmacological target for preventing and treating cancer disease mainly in colorectal cancer. Thus far, therapeutic strategies have focused on selective inhibitors of COX-2 activity; however, less attention has been paid

to identifying anticancer agents that suppress the expression of COX-2. The 5'-untranslated region of the COX-2 gene contains binding sites for numerous regulatory transcription factors including two nuclear factor- $\kappa$ B motifs, two activator protein 1 sites and two cAMP-response elements (CREs) among other.<sup>14</sup> However, the regulation of the expression of COX-2 is much more complex; it is known that COX-2 expression is also regulated by genomic DNA and chromatin modifications and by post-transcriptional regulation via its 3'-untranslated region.<sup>15</sup>

DNA methylation and histone modifications represent the major epigenetic mechanisms implicated in the regulation of gene transcription in mammals. COX-2 promoter contains numerous CpG islands that, when hypermethylated, result in transcriptional silencing and this regulates the survival of carcinoma cells and affects clinical outcomes in gastric cancer.<sup>16,17</sup> The COX-2 promoter activation by inflammatory mediators in human fibroblasts and mouse macrophages is mediated by the histone acetyltransferase p300/CBP-associated factor.<sup>18</sup> Diminished COX-2 expression in fibroblasts due to epigenetic abnormality in the form of histone hypoacetylation has a key role in the pathogenesis of idiopathic pulmonary fibrosis.<sup>19</sup> Recently, it has been reported that induction of COX-2 by hepatitis B virus depends on the demethylation of the COX-2 promoter by downregulating the DNA methyltransferase 3B and the increased binding of transcription factors.<sup>20</sup>

In this work, we have monitored the epigenetic marks (that is, DNA methylation and histone acetylation) at the COX-2 promoter in hepatoma cell lines and HCC biopsies. The results shown in this study suggest that the reduced COX-2 expression in some hepatoma cell lines and HCC is closely associated with the

<sup>1</sup>Instituto de Biomedicina de Valencia, IBV-CSIC, Valencia, Spain; <sup>2</sup>Instituto de Investigaciones Biomédicas Alberto Sols, CSIC-UAM, Madrid, Spain and <sup>3</sup>Centro de Investigación Biomédica en Red de Enfermedades Hepáticas y Digestivas (CIBERehd), Barcelona, Spain. Correspondence: Dr M Casado, Instituto de Biomedicina de Valencia, IBV-CSIC, Jaime Roig 11, 46010 Valencia, Spain or Dr P Martín-Sanz, Instituto de Investigaciones Biomédicas Alberto Sols, CSIC-UAM Arturo Duperier, 4 28029 Madrid, Spain. E-mail: mcasado@ibv.csic.es or pmartins@iib.uam.es

<sup>4</sup>These authors contributed equally to this work.

Received 30 March 2012; revised 11 June 2012; accepted 14 June 2012

methylation status and histone deacetylation. Treatment with demethylating agents or histone deacetylase (HDAC) inhibitors restored the expression of COX-2. In agreement with these data, a reduction of overall survival (OS) of the patients was observed after decreased COX-2 expression by promoter hypermethylation and histone H3 hypoacetylation.

## RESULTS

### COX-2 expression and protein levels in HCC cell lines

COX-2 mRNA and protein levels were analyzed in six human cell lines using human hepatocytes as control. WRL68, which is derived from the human liver embryo, exhibited the highest COX-2 mRNA expression whereas HepG2 and HuH-7 liver carcinomas showed low levels of COX-2 mRNA and protein (Figures 1a and b). Prostaglandin E<sub>2</sub> levels, measured in cell supernatants, correlate with COX-2 protein levels (Figure 1c).

### Methylation analysis of COX-2 promoter in hepatic cell lines

It has been suggested that hypermethylation of certain CpG sites on COX-2 promoter results in transcriptionally silencing and this regulates the growth of carcinoma cells.<sup>17,21,22</sup> The MethPrimer analysis of the COX-2 genomic region organizes the CpG sites in the 5' region into three CpG islands (Figure 2a). The first two islands (A and B) are located in the promoter region and they do not overlap with previously identified binding sites (C/EBP, nuclear factor of activated T-cells or AP1).<sup>23</sup> The third one (C) covers a domain including the CRE-binding site with a main function in transcriptional regulation, the first exon, including both the coding and noncoding regions, and the initial part of the first intron.

We analyzed first by methylation-sensitive restriction assay (MSRA) the methylation state in several CpG sites to assess if there was a correlation between methylation signatures and COX-2 expression in different hepatic cell lines as compared with the human liver. HuH-7 and CHL cells, as well as the human liver, presented a non-methylation pattern along the studied region. Although different patterns were found in all the cell lines analyzed, no correlation between CpG methylation and the COX-2 mRNA levels was observed, even considering separately each CpG site (Figure 2b). We further quantified the methylation size by sequencing 6, 8 and 20 CpGs on the CpG islands A, B and C, respectively (Figure 2c). The pyrosequencing data are in accordance with the MSRA results. The first two CpG islands were remarkably hypermethylated in Hep3B and HuH-6, while they remained unmethylated in CHL and WRL68 cells. Moreover, HepG2 and HuH-6 but not HuH-7 cells presented a hypermethylation pattern in CpG island C. In this region, Hep3B and CHL presented a low methylation profile. The analysis of a pool of control human liver DNA showed that normal liver presents unmethylated CpGs all along this region. The results obtained by both assays indicate that it is not possible to predict the basal

expression of COX-2 from the methylation data. The WRL68 cell line, which presents the highest levels of COX-2 expression, showed the same methylation profile than the human liver or HuH-7 cells, both with negative expression levels.

We then analyzed by pyrosequencing the effect of the demethylating agent 5-aza-2'-deoxycytidine (AzadC) on COX-2 CpG islands. The percentage of COX-2 global CpG islands methylation decreased from 80 to 59% in HuH-6, and from 43 to 33% in Hep3B cells after AzadC treatment (Figure 3a). No decrease was observed in HuH-7 cells that presented a low

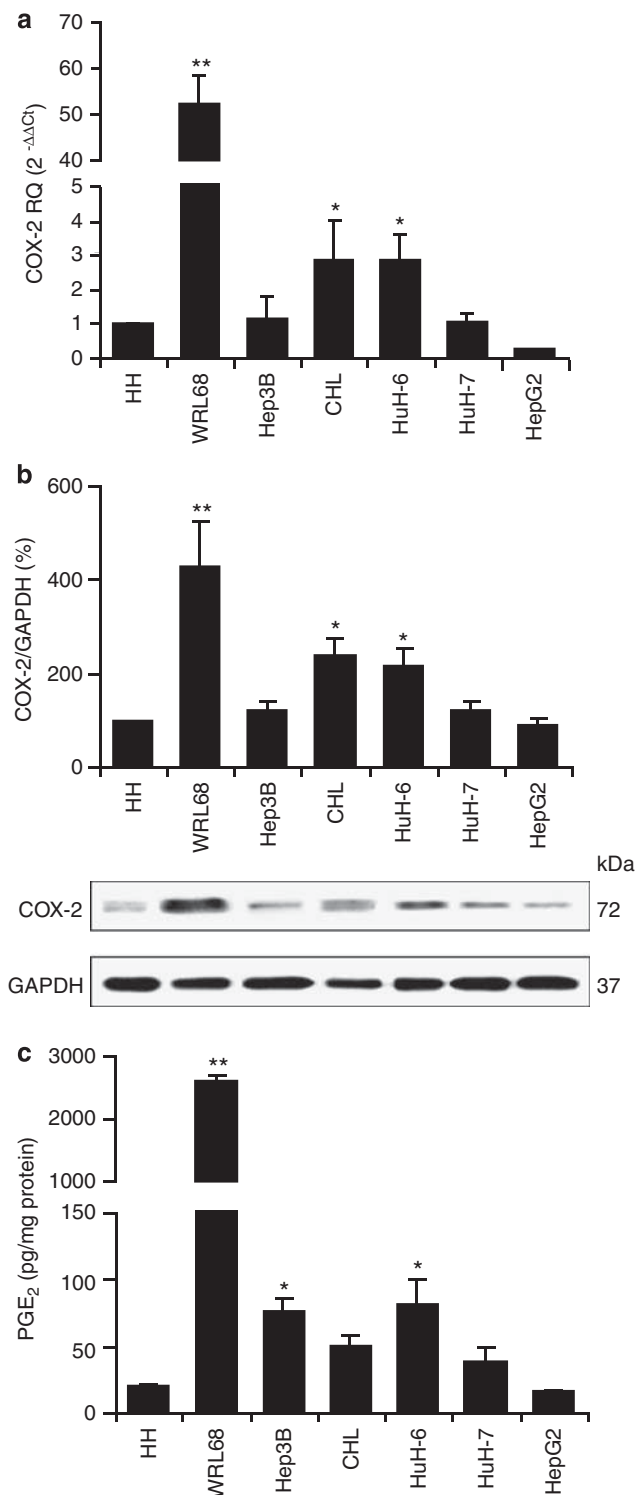


**Figure 1.** COX-2 expression and protein levels in HCC cell lines. Cells were plated in 100-mm dishes and grown to 60–70% confluence in a culture medium supplemented with 10% fetal bovine serum. **(a)** Total RNA was prepared from hepatic cell lines and COX-2 mRNA was analyzed by quantitative PCR. COX-2 mRNA amounts were calculated as relative quantitation (RQ) and normalized to the expression of 18S levels. Values represent fold change relative to human hepatocytes (HH). **(b)** Total cellular extracts were prepared from hepatic cells and protein (50 μg per lane) was analyzed by western blot. A representative western blot out of four is shown. The expression of target protein was normalized to that of GAPDH. Densitometric analysis of COX-2 expression using HH as reference control (100%) is also shown **(c)** Prostaglandin E<sub>2</sub> (PGE<sub>2</sub>) concentration was determined by enzyme immunoassay in the supernatant of the cells. Data are reported as means ± s.d. of four independent experiments. \**P* < 0.05 and \*\**P* < 0.01 vs HH.

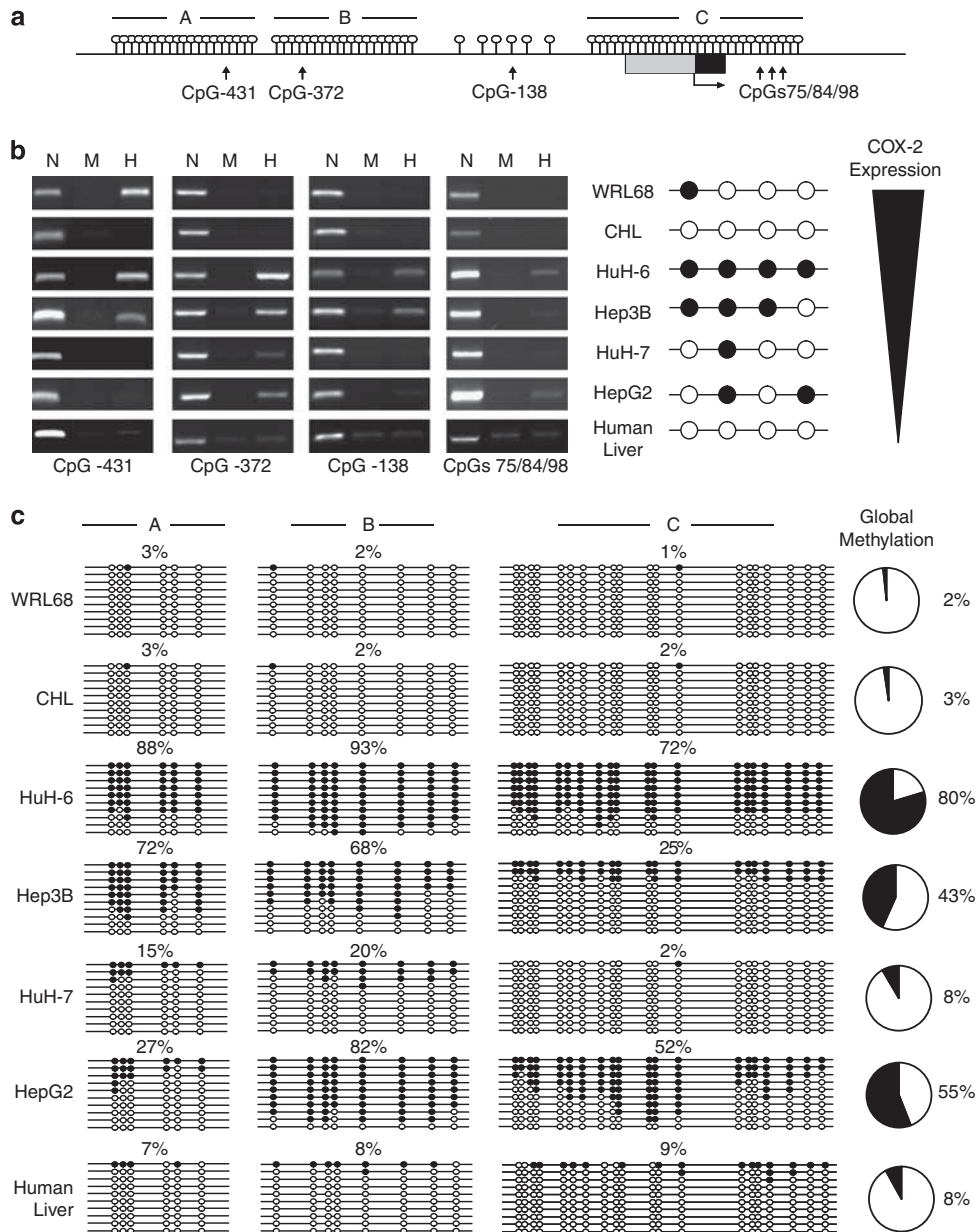


**Figure 2.** Methylation analysis of CpG islands at COX-2 gene in HCC cells. **(a)** Representative scheme of putative CpG islands (A, B, C) identified by bioinformatic analysis and CpG dinucleotides detected by MSRA (black arrows) in the 5' upstream region of COX-2 gene. The non-coding (gray rectangle) and coding (black rectangle) regions of the first exon are also shown. **(b)** The MSRA technique was used to analyze the methylation profile of CpG sites in the COX-2 promoter region using DNA from the human liver and six liver derived cell lines. DNA digested with *MspI* (M), *HpaII* (H) or no restriction enzyme (N) was amplified by PCR using primers recognizing the - 431, - 372, - 138 or 75/84/98 CpG sites. A representative ethidium bromide-stained agarose gel is shown for each PCR reaction. A scheme of methylation state is represented using white balls (non-methylated) or black balls (methylated). The COX2 expression levels in the cell lines are represented with a black triangle. **(c)** Profiles of the percentage of methylation in the each CpG (A, B, C) islands of COX-2 promoter in the human liver and hepatic cell lines analyzed by bisulfite pyrosequencing. The global promoter methylation percentage for each sample is shown in the right panel.

methylation percentage in basal conditions. In the same conditions, COX-2 mRNA levels were analyzed by reverse transcription-quantitative PCR. HuH-6 and Hep3B presented a 5- and 78-fold induction of COX-2 expression, respectively. Furthermore, HuH-7 cells presented a fourfold induction of COX-2 expression after treatment with AzadC despite the absence of changes in the methylation pattern (Figure 3b), highlighting the relevance of promoter demethylation in the regulation of COX-2, although other alternative mechanisms may coexist. To assess if this differential response is a specific mechanism related to COX-2 regulation, we determined the amount of glyceraldehyde-3-phosphate dehydrogenase (GAPDH) mRNA normalized to the

expression of 18S in all cell lines used. AzadC produced a minor reduce in GAPDH expression, with an effect that was quantitatively comparable in the three cell lines analyzed.

#### Role of histone acetylation on COX-2 transcription in HCC cells

To evaluate the effect of histone modifications on COX-2 expression, we first examined the effects of two HDAC inhibitors (HDACis), sodium butyrate (NaB) and suberoylanilide hydroxamic acid (SAHA), on COX-2 mRNA and protein levels in hepatic cell lines. Treatment of cells with the inhibitors promoted a marked increase of COX-2 mRNA levels at 16 h (no changes were found at

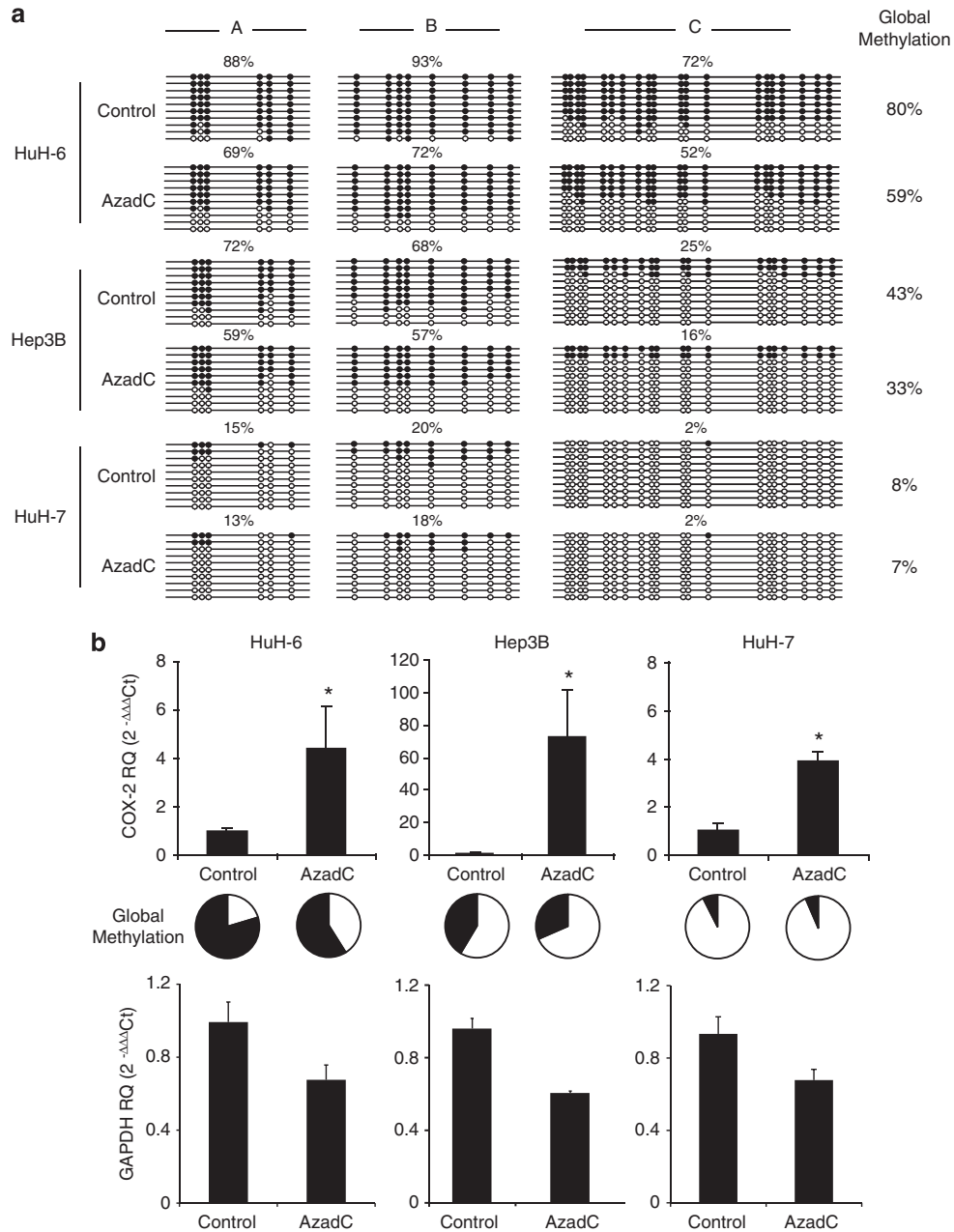


**Figure 3.** Effect of the demethylating agent, AzadC, on the methylation state in COX-2 CpG islands. **(a)** Methylation percentage profiles of each COX-2 promoter CpG (A,B,C) islands in HuH-6, Hep3B and HuH-7 cells in control or 5  $\mu$ M AzadC-treated cells analyzed by bisulfite pyrosequencing. The global promoter methylation percentage for each condition is shown in the right panel. **(b)** COX-2 mRNA in HuH-6, Hep3B and HuH-7 control and AzadC-treated cells by quantitative PCR. COX-2 and GAPDH mRNA amounts were calculated as RQ and normalized to the expression of ribosomal 18S. Values represent fold change relative to control condition in each cell line. The global CpG methylation for each cell line and condition is also shown. \* $P < 0.05$  vs the corresponding cell line without treatment.

6 h) except for WRL68 (Supplementary Figure S1). A significant increase in COX-2 was observed in Hep3B, HuH-6 and HuH-7 hepatoma cells by the effect of both NaB and SAHA after 24 h of treatment (Figure 4a). Prostaglandin  $E_2$  levels well correlated with COX-2 protein (Figure 4b). No changes were detected in HDAC1, 2, 3 and SIRT1 protein levels by the effect of HDACis in HCC cells. The acetylation status of histone H3 and histone H4 was evaluated (Figure 4a) and a significant increase in acetylated histones H3 and H4 was observed in HCC cells. Moreover, when global HDAC activity was measured by using a colorimetric detection assay, the highest activity corresponded to Hep3B and HuH-6 cells. As expected, global HDAC activity was inhibited by treatment of the

cells with NaB and SAHA (Figure 4c). These results suggest that histone acetylation regulates COX-2 expression in some HCC cells.

We determined whether there was a direct link between the increased H3 and H4 acetylation and COX-2 expression, analyzing the effects of NaB on acetylated histones recruitment at the COX-2 promoter. We ascertained the interaction of Ac-H3 and Ac-H4 all along the 5' region of the COX-2 human gene using a standard chromatin immunoprecipitation assay followed by real-time PCR. The  $\alpha$ -RNA polymerase antibody was used as a control of gene activity. Four different primer pairs were used to cover the complete regulatory sequence starting on a distal promoter region, and ending on the first intronic region. We found an



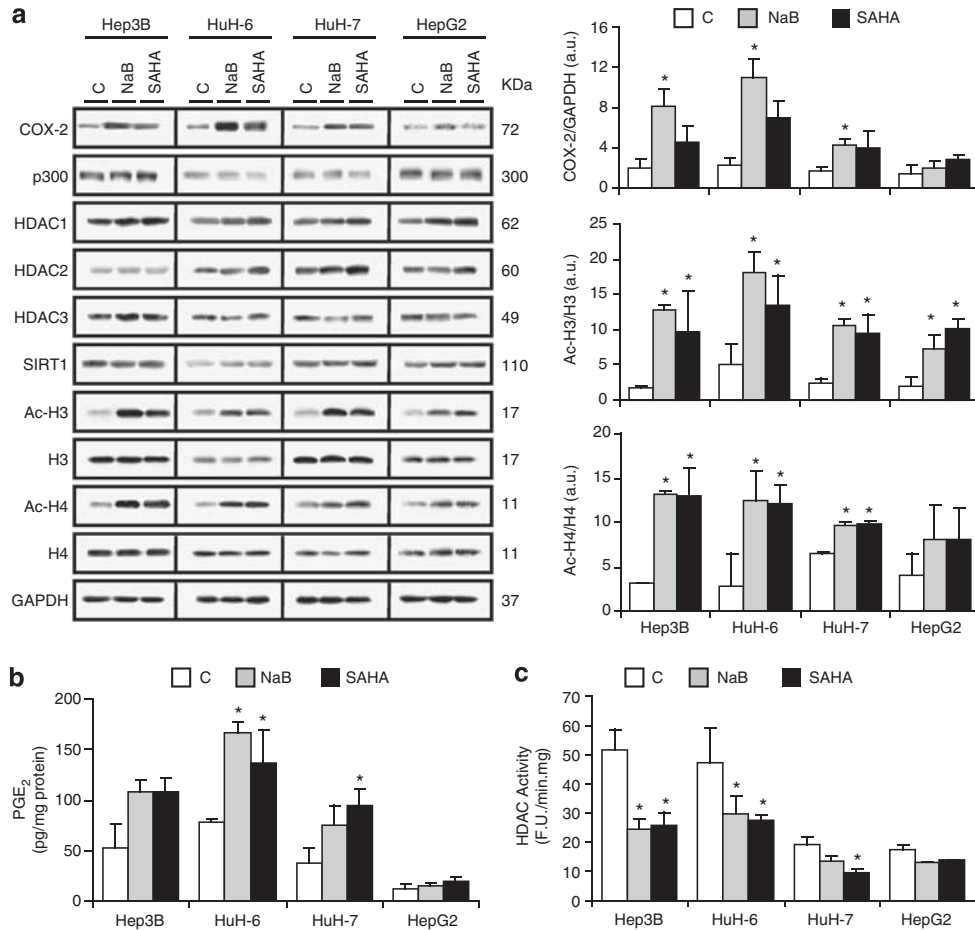


**Figure 4.** COX-2, HDACs and acetylated H3 and H4 protein levels after treatment of HCC cells with HDACis. **(a)** HCC cells in 1% fetal bovine serum were incubated without (white) or with 2.5 mM NaB (gray) or 2.5 μM SAHA (black) for 24 h. Cellular extracts were prepared and protein was analyzed by western blot. Left panel shows a representative western blot analyzing COX-2, p300, HDAC1, 2, 3, SIRT1 and acetylated (Ac) or total histones H3 y H4 protein levels. Each panel has an optimal exposition time. Results are expressed as arbitrary units after densitometric analysis of COX-2 expression or the expression of the ratios Ac-H3/H3 and Ac-H4/H4 normalized to GAPDH (right panel). **(b)** Prostaglandin E<sub>2</sub> (PGE<sub>2</sub>) concentration was determined by enzyme immunoassay in the supernatant of the cells. **(c)** Global HDAC activity was measured by using a fluorimetric detection assay as described in Materials and Methods and the results are expressed as fluorescence units (FU) per minute and mg of protein. Data are expressed as means ± s.d. of three independent experiments. \**P* < 0.05 vs the corresponding cell line without treatment.

increased Ac-H3 association both in HuH-6 and HuH-7 cells, with a higher signal in HuH-6 cells after treatment with NaB. The increased association is higher in the proximal promoter and the noncoding part of the first exon, which includes the CRE regulatory site. An increased Ac-H4 association was only seen on HuH-6 cells chromatin (Figure 5a).

To investigate whether histone acetylation is associated with HCC, we determined the COX-2, histone H3 and acetylated-H3 immunoreactivity in tumor tissue samples. Ac-H3 staining was observed primarily in the cell nuclei (Figure 5b). Immunoreactivity of Ac-H3 protein ranged from 138% to 34% vs a positive control tissue (amygdala) considered as 100%.<sup>24</sup> In the study cohort, high expression of Ac-H3/H3 ratio was detected in 67% of HCCs. Assessment of survival in these patients revealed that high Ac-H3/H3 ratio was correlated with a favorable disease-specific survival (*P* = 0.021; Figure 5c). Moreover, an increased COX-2 immunoreactivity was observed in the tumors with a major Ac-H3/H3 ratio (Figure 5b).

It has been described that demethylating agents and HDACs function in synergy by depleting methyltransferase activity and reversing the formation of transcriptionally repressive chromatin structure.<sup>25,26</sup> Combined treatment with AzadC and NaB or SAHA induced a higher increase of functional COX-2 protein levels than

the HDACis alone. Moreover, both drugs decreased DNMT1 protein levels in HCC cells (Supplementary Figure S2).

#### Methylation analysis of COX-2 promoter in primary HCCs

Quantitative real-time RT-PCR analysis of HCC samples revealed significantly higher COX-2 mRNA levels vs normal human liver. Moreover, 86% patients showed a higher COX-2 expression in the non-tumoral biopsies compared with their paired tumoral sections (Figure 6b), as it has been described previously.<sup>12</sup> To determine whether aberrant methylation of COX-2 is associated with HCCs, we performed bisulfite sequencing of CpG islands A, B and C at COX-2 locus from 23 tumor and non-tumor clinical samples of HCC patients. Consistent with the expression levels, the COX-2 promoter was methylated extensively in tumor tissues compared with the corresponding nontumor sections (Figure 6c). However, the hypermethylation of COX-2 promoter was exclusively found in 57% of the tumor tissues with respect to their non-tumor counterparts (Figure 6a). The average global methylation in these samples was 31% and 7.6% of tumor and non-tumor tissues, respectively. In all cases, the altered methylation pattern was clearly seen in the CpG islands B and C but not in the A. Next, we investigated whether this differential methylation status was

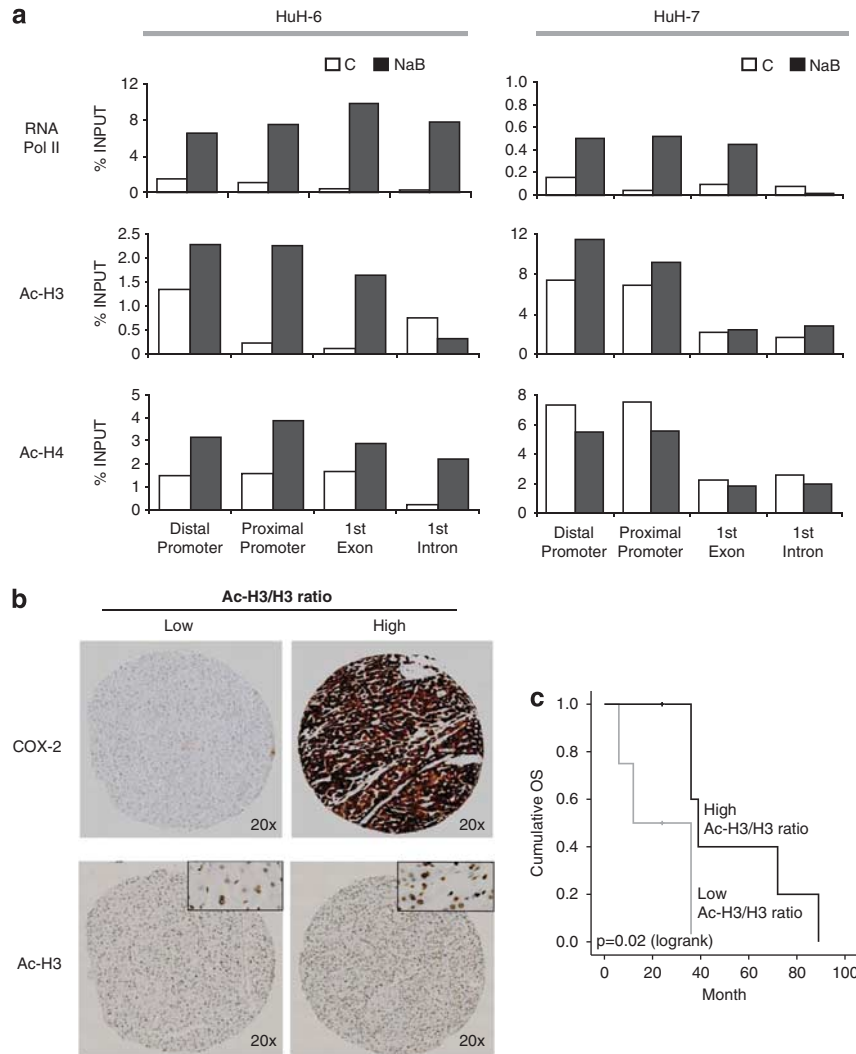


**Figure 5.** Effect of HDACis on histone H3 and H4 acetylation at the human COX-2 promoter in HCC cells. Role of acetylation in primary HCCs. **(a)** Chromatin immunoprecipitation assay was performed with HuH-6 and HuH-7 cells in control (white bars) or NaB (black bars)-treated conditions. Immunoprecipitation of samples was performed with anti-acetylated histone antibodies. The histone binding was analyzed using oligonucleotides that recognize different parts of the 5' regulatory region of the COX-2 gene. A positive control of transcriptionally active genes was performed using anti-RNA-polymerase II antibody and a negative control with no antibody. The results are representative of three quantitative PCR independent experiments. **(b)** Immunohistochemical staining of COX-2, acetylated histone H3 (Ac-H3) in HCCs. Original magnification  $\times 20$ . Expression of COX-2 and Ac-H3 was shown in representative HCC patients according immunoreactivity levels. Inset: Positive staining of Ac-H3 in nuclei ( $\times 80$ ). **(c)** Kaplan-Meier survival analysis of Ac-H3/H3 ratio in subsets of HCC patients with a different percentage ratio:  $\leq 50\%$  (low; gray line) or  $> 50\%$  (high; black line) relative to the ratio in the positive control tissue (100%).

correlated with COX-2 expression in clinical samples of HCC. A statistically significant inverse association was observed between the COX-2 mRNA levels and methylation status in HCC (Figure 6d). Moreover, OS was significantly different according to the methylation status without significant differences in disease-free survival rates (Figure 6e). A hypermethylation of COX-2 promoter was significantly associated with a poor OS ( $P = 0.04$ ). We did not observe any significant association with other clinical signs (Table 1).

## DISCUSSION

Increased COX-2 expression has been found in the early stages, but is lost in advanced HCC.<sup>13</sup> Moreover, COX-2 mRNA levels were significantly higher in the adjacent healthy liver than in HCC and lower in HCC than in nonalcoholic steatohepatitis disease.<sup>27</sup> Therefore, many questions remain unsolved regarding the

contribution of COX-2 to induce/regulate tumorigenesis. As the mechanisms regulating COX-2 expression at specific stages of HCC progression remain unknown, we hypothesize that COX-2 expression could be regulated by epigenetic changes such as DNA methylation and histone acetylation. Here, we show that the low COX-2 expression in some HCC lines and in HCC biopsies is associated with COX-2 promoter hypermethylation and histone deacetylation. Conversely, treatment with HDACis or demethylating agents increased the expression of COX-2.

DNA methylation is a predominant mechanism used to inactivate relevant genes during HCC tumorigenesis. Recent findings support the hypothesis that hypomethylation of the DNA surrounding the proximal promoter region is a prerequisite for activation of oncogenes, whereas hypermethylation leads to gene silencing of putative tumor-suppressor genes.<sup>28</sup> The therapeutic and chemopreventive significance of methylation patterns in human HCC have been reported; Lee *et al.*<sup>29</sup> showed

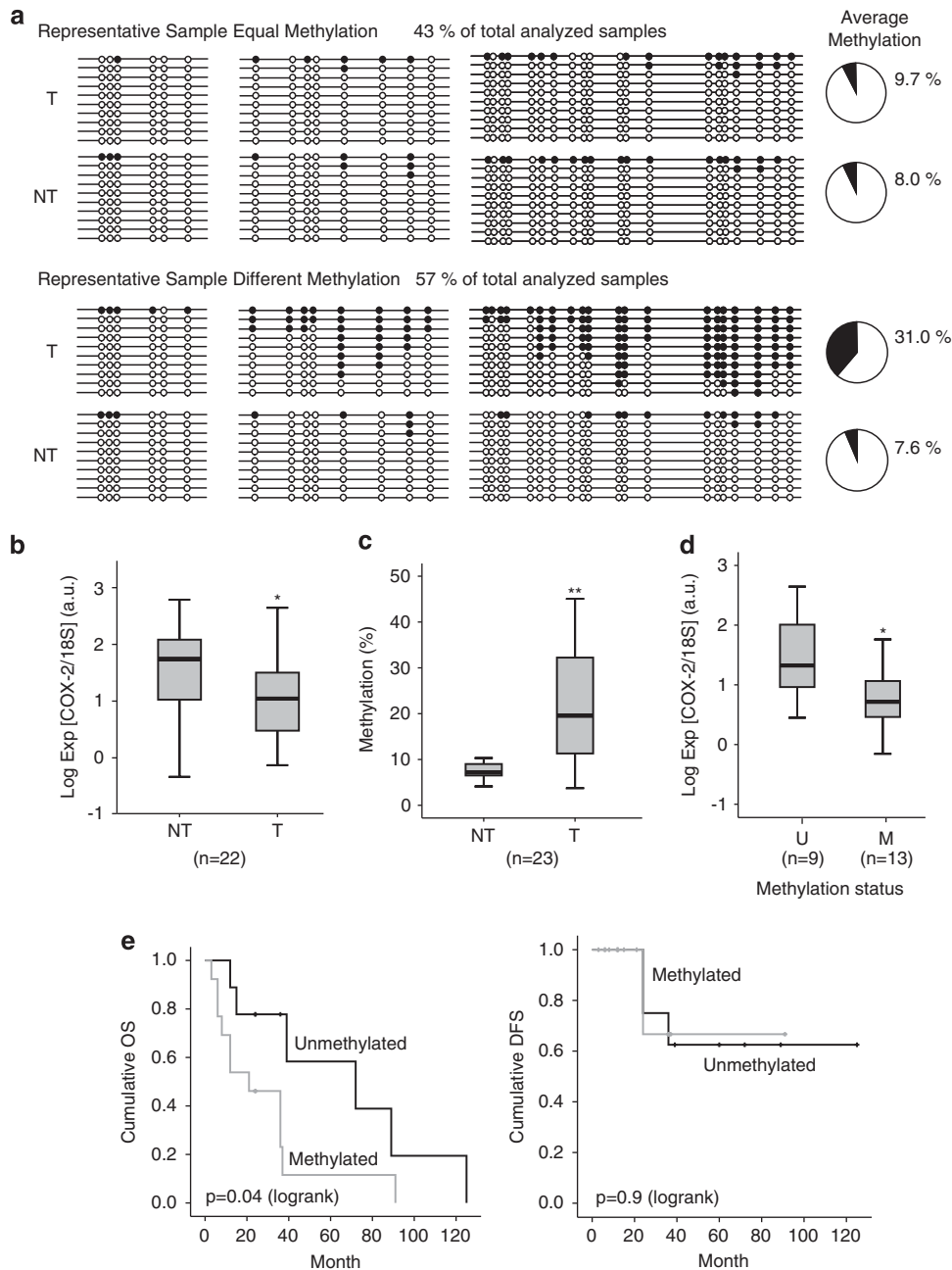


**Figure 6.** Methylation analysis of COX-2 promoter in primary HCCs. **(a)** DNA methylation status of the COX-2 promoter in HCC tumor (T) and non-tumor (NT) samples determined by bisulfite pyrosequencing. A representative scheme of equal or altered methylation status between tumor (T) and non-tumor (NT) biopsies is shown. The global promoter methylation percentage for each group is shown in the right panel. **(b)** COX-2 mRNA levels in liver tissue from 23 patients were determined by quantitative real-time RT-PCR using 18S as the normalization control. NT, T ( $n = 22$ ). \* $P < 0.05$  vs NT samples; **(c)** Methylation quantities were determined by pyrosequencing ( $n = 23$ ). \*\* $P < 0.01$  vs NT samples **(d)** Box plots showing the analysis of the association between COX-2 mRNA levels and methylation status. The samples were classified according the average methylation of COX-2 promoter between tumor and their non-tumor counterparts. U, samples exhibited a low percentage of COX-2 promoter methylation without differences between the tumoral and non-tumoral tissue ( $n = 9$ ); M, patients showed a higher percentage of COX-2 promoter methylation in the tumoral tissue ( $n = 13$ ). **(e)** OS and disease-free survival (DFS) curves according to COX-2 methylation status using Kaplan–Meier survival plots. OS is significantly associated with the methylation status of COX-2 ( $P = 0.04$ ). Gray line, patients with a hypermethylation status in the tumoral tissue; black line, patients without alteration in percentage of methylation of COX-2 promoter between tumor and their non-tumor counterparts.

that the *APC*, *GSTP1*, *RASSF1A*, *p16*, *COX-2* and *E-cadherin* genes were frequently methylated in HCC. Moreover, *COX-2*, *p16*, *RASSF1A* and *TIMP-3* were not methylated in liver cirrhosis and chronic hepatitis from patients without concurrent HCC. To date, frequent and aberrant methylation of *Ras* and Janus kinase/signal

transducer and activator of transcription inhibitors in HCC resulted in persistent activation of the *Ras* and Janus kinase/signal transducer and activator of transcription pathways.<sup>30</sup> The same group<sup>31</sup> has investigated the global levels of DNA methylation as well as the methylation status of 105 putative tumor-suppressor

**Table 1.** Clinicopathological features of 23 HCC patients

	Methylation status of tumor biopsies		P
	Unmethylated	Methylated	
Sex			0.339
Male	9	9	
Female	1	4	
Age	70.2 ± 7.2	63.46 ± 15.6	0.284
Etiology			0.709
HBV	1	1	
HCV	4	4	
Ethanol	1	3	
HCT	1	0	
NA	3	5	
Cirrhosis			0.673
Positive	3	5	
Negative	7	8	
Tumor size			0.372
> 5	2	6	
< 5	6	6	
NA	2	1	
Histological grade			0.282
WD	5	9	
MD	3	3	
UD	0	1	
NA	2	0	

Abbreviations: HBV, hepatitis B infection; HCC, human hepatocellular carcinoma; HCT, Hemochromatosis; HCV, hepatitis C infection; MD, moderate differentiated; NA, not assigned; UD, undifferentiated; WD, well differentiated.

genes and found that the extent of genome-wide hypomethylation and CpG hypermethylation correlates with biological features and clinical outcomes of HCC patients. Furthermore, methylation also appears to be an early event, suggesting that this may precede cirrhosis. The more aggressive subclass A of HCC displayed a very high frequency of gene promoter hypermethylation, a condition similar to the CpG island methylator phenotype described in human colorectal cancer.<sup>32</sup> Recently, Yang *et al.*<sup>33</sup> have identified genes whose methylation and mRNA levels are associated with recurrence after resection for HCC using integrated analysis by whole-genome DNA methylation and mRNA expression data. They suggest that potential novel oncogenes (*PSRC1*, *MYO1E*), tumor-suppressor genes (*CFH*, *MYRIP*) and TGF, Wnt and cytoskeletal remodeling were the major pathways enriched with the recurrence predicting genes. Regarding COX-2, it has been reported that epigenetic silencing of COX-2 affects clinical outcome in gastric cancer.<sup>16</sup>

To clarify the methylation status of the COX-2 promoter in HCC three CpG islands, identified through bioinformatic analysis, were examined by pyrosequencing in six hepatic cell lines exhibiting different COX-2 expression levels. Furthermore, CpG sites located at -431, -372, -138 and +75/84/98 were analyzed by the MSRA analysis. We observed a broad range of methylation from 2% in WRL68 to 43% in Hep3B cell line, without a correlation between these percentages and COX-2 expression. Nevertheless, we could demonstrate that treatment with a demethylating agent, AzadC, readily induced COX-2 expression in HCC cells. These results suggest that the methylation status of the promoter can regulate COX-2. However, we could not discard indirect mechanisms regulating COX-2 expression, as observed in HuH-7 cells, in which the treatment with demethylating agent increased the COX-2 mRNA levels despite the permanent hypomethylation

status of the promoter in this cell line. In fact, it has been suggested that in colorectal cancer cells, AzadC is capable of influencing other factors involved in gene expression such as proteins with a methyl-binding domain or histone modifications.<sup>34</sup>

Prostaglandin E<sub>2</sub> promotes intestinal tumor growth via DNA methylation of certain tumor-suppressor and DNA-repair genes by enhancing their promoter methylation.<sup>35</sup> Moreover, hypermethylation of COX-2 gene promoter has been identified as an independent prognostic factor in gastric cancer patients.<sup>16</sup> These results prompted us to study whether the methylation of COX-2 promoter was related with the COX-2 expression in HCC. In agreement with previous work,<sup>9,36</sup> COX-2 mRNA levels were higher in the adjacent liver tissue than in HCC in the 86% of the studied biopsies. When we analyzed the methylation profile at three CpG islands, we could classify the samples in two groups: 43% of samples exhibited a low percentage of COX-2 promoter methylation without differences between the tumoral and non-tumoral tissue, whereas the remaining 57% showed a higher percentage of COX-2 promoter methylation in the tumoral tissue. This methylation status was associated with COX-2 expression as suggested by the significant differences in the levels of COX-2 between both groups. These results suggest that the promoter hypermethylation is an important regulatory mechanism of COX-2 expression in HCC.

The long-term survival of patients with HCC is unsatisfactory, in part because of the high rate of recurrence after curative surgical resection of hepatocellular carcinoma. There have been many reports on the prognostic significance of epigenetic alterations at the promoter region of genes associated with HCC. For example, patients with E-cadherin or GSTP1 methylation showed poorer survival than those without.<sup>29</sup> In this study, COX-2 methylation was associated with poor prognosis in HCC. Although it remains unclear how COX-2 methylation affects prognosis in these cases, methylation of COX-2 may occur concordant with other methylation alterations and could be part of the genome-wide methylation defect in these cancers.<sup>37</sup> Thus, COX-2 may integrate a CpG island methylator phenotype associated with poor prognosis.

NaB, a short-chain fatty acid that is normally present in the human colon as a product of the metabolic degradation of complex carbohydrates, was the first compound found to possess histone deacetyltransferase-inhibiting activity.<sup>38</sup> Different pre-clinical studies with NaB showed its ability to inhibit HCC cell growth. Beside NaB, hydroxamic acids including trichostatin A and SAHA are undergoing phase I and II clinical trials to validate their potential use as anticancer drugs for solid and hematological tumor treatment either as monotherapies or in combination with other cytotoxic agents. Our data demonstrate that treatment of HCC cells with NaB or SAHA increased COX-2 expression and restored acetylation of histones H3 and H4 around COX-2 promoter in some hepatoma cell lines. An interesting finding in our study was that HCC patients with a major percentage of histone H3 acetylation had a better survival. Thus, it is speculated that epigenetic mechanism that implies a less expression of COX-2 are linked to poor prognosis of patients with hepatocarcinoma.

There are some different results concerning the effect of HDACis on COX-2 expression. To date, butyrate and trichostatin A suppress COX-2 expression in HT-29 cells by inhibition of RNA polymerase II elongation on the COX-2 gene and the same occurs for c-myc.<sup>39</sup> In KYSE450 (esophageal squamous cell carcinoma) and in 184B5/HER (Neu-transformed breast cells), HDACis suppress PMA-mediated induction of COX-2<sup>40</sup> and in human non-small cell lung cancer cells, trichostatin A-induced apoptosis and decreased the levels of COX-2 mRNA and protein expression.<sup>41</sup> However, NaB and trichostatin A accentuated LPS-induced COX-2 gene expression through mitogen-activated protein kinase-dependent increase of phosphorylation and acetylation of histone H3 at the COX-2 promoter and by decreasing C/EBP $\delta$  levels.<sup>42,43</sup> These



results and our data suggest that the effect of HDACis on COX-2 activation does not appear to be common to all the cell types and even not related with their anti-tumoral activity.

In conclusion, COX-2 expression appears to be regulated at first instance by promoter methylation and histone acetylation in hepatoma cell lines and HCC. Our results indicate that alterations in promoter methylation of COX-2 occur exclusively in hepatic tumor regions of HCC and that aberrant methylation of COX-2 in HCC leads to poor prognosis after surgical resection. Primary tumor COX-2 methylation status may therefore be used as a signature to decide a more aggressive treatment in HCC. Our data suggest that epigenetic mechanisms that imply reduced COX-2 expression are linked to poor prognosis of HCC patients. The identification of the crosstalk between epigenetic signatures and transcription factors activity appears to be relevant for the implementation of new HCC therapeutic approaches.

## MATERIALS AND METHODS

### Cell lines and tissue samples

A total of 23 individual tumoral and paired non-tumoral frozen HCC tumors were obtained from the de Spanish Tumor Bank Network of the Centro Nacional de Investigaciones Oncológicas. Institutional Review Board approval was obtained for these studies and all participants provided written informed consent. All tissues were evaluated by pathologists by means of hematoxylin/eosin staining. Histological graded as well (WD), moderate (MD) or undifferentiated (UD) was determined according to the Edmondson and Steiner classification, following World Health Organization recommendations. Clinicopathological parameters of HCC patients are summarized in Table 1. This retrospective cohort study used a prospective database during 8-year period (partial liver resection from 2001 to 2009, follow-up data until 2011). Death from any cause was used to determine the OS rate. Disease-free survival was defined as a patient who was alive at the end of the follow-up period. All specimens examined in this study were collected at primary surgery. At the time of the last follow-up 5 (21.7%) patients were alive and 18 (78.3%) patients had died of disease (median OS 44.2 months, confidence interval 95% = 27–61%).

The human liver cell lines WRL68, Chang liver (CHL) and the hepatoma cell lines HepG2 and Hep3B were purchased from the American Type Culture Collection (ATCC, Manassas, VA, USA). All these cell lines were authenticated by ATCC and were expanded twice, and stored in liquid N<sub>2</sub>. Expansions from these clones were used up to 6 months in culture. HuH-6 and HuH-7 cell lines were kindly provided by Dr Perret (Institut Cochin, CNRS UMR8104, University Paris-Descartes, Paris, France) and Dr Kern (Department of General Pathology, University Hospital Heidelberg, Heidelberg, Germany), respectively. Cells were grown on Eagle's Minimal Essential Medium or Dulbecco's modified Eagle's medium (Sigma Chemical Co. St Louis, MO, USA) supplemented with 10% fetal bovine serum and antibiotics (50 µg each of penicillin, streptomycin and gentamicin per ml). The cells were treated with the following drugs alone or in combination: 2.5 mM NaB (Sigma), 2.5 µM SAHA (Sigma) and 5 µM 5-aza-2'-deoxycytidine (AzadC; Sigma). Timing and concentration curves were performed previously to determine the optimal concentrations.

### RNA extraction and quantitative real-time PCR analysis

Total RNA from single-freeze cryopreserved pooled human hepatocytes (HPCH10 CryostaX, XenoTech, Lenexa, KS, USA), cell lines and liver biopsy samples was extracted by using TRIzol reagent (Life Technologies, NY, USA). RNA (1 µg) was reverse transcribed using a Transcriptor First Strand cDNA Synthesis Kit following the manufacturer's indications (Roche Applied Science, Indianapolis, IN, USA). The cDNA was used as template for real-time PCR through Taqman probes. COX-2 (Hs00153133\_m1), GAPDH (Hs99999905\_m1) or 18S (Hs99999901\_m1) assay on demand gene expression products were used (Life Technologies). Real-time PCR was performed using a MyiQ detection system (Bio-Rad Laboratories, Hemel Hempstead, UK) and thermocycling parameters were 95 °C for 10 min, 50 cycles of 95 °C for 15 s followed for 60 °C for 1 min. Each sample was run in triplicate and was normalized to 18S levels. Three replicates were then averaged, and fold induction was determined in a  $\Delta\Delta C_t$  based fold-change calculations.

### Western blot analysis

Extracts from cells ( $2-3 \times 10^6$ ) or cryopreserved pooled human hepatocytes were obtained as described previously.<sup>44</sup> The relative amounts of each protein were determined with the following polyclonal or monoclonal antibodies: COX-2 (sc-1747, Santa Cruz Biotechnology, Santa Cruz, CA, USA); HDAC 1, 2, 3 (Santa Cruz and Cell Signaling, Boston, MA, USA); sirtuin 1 (SIRT1; Millipore, Billerica, MA, USA); anti-histone 3 (H3), anti-histone 4 (H4) and anti-acetylated H4 (Ac-H4; Abcam, Cambridge, UK); anti-acetylated H3 (Ac-H3; Millipore) and DNA (cytosine-5) methyltransferase 1 (DNMT1; Imgenex, San Diego, CA, USA). After incubation with the corresponding anti-rabbit or anti-mouse horseradish peroxidase-conjugated secondary antibody, blots were developed by the ECL protocol (GE Healthcare, Chalfont St Giles, UK). Target protein band densities were normalized with the expression of GAPDH (Life Technologies). The blots were revealed, and different exposition times were performed for each blot with a charged coupling device camera in a luminescent image analyzer (Chemi-Doc XRS, Bio-Rad) to ensure the linearity of the band intensities. Densitometric analysis was expressed in arbitrary units.

### Immunohistochemical staining

Two- to four-micrometer thick paraffin-embedded tissue microarrays and complete sections were cut onto Dako slices (Dako, Glostrup, Denmark) by Immunohistochemistry unit of the Centro Nacional de Investigaciones Oncológicas, and subsequently dewaxed, rehydrated and subjected to antigen retrieval by heating in PTLINK with 50 mM Tris/EDTA pH 9.0. The slides were cooled and treated with peroxidase-blocking solution (Dako) for 5 min. Sections were immunostained with a COX-2 antibody (NeoMarkers, Suffolk, UK), anti-histone H3 (Abcam) and acetyl-histone H3 (K9; Abcam) in a Autostainer Plus (Dako). In parallel, each tissue section was also incubated with a rabbit anti-mouse antiserum and was used as a negative control. Microphotographs were taken with an EnVision FLEX system (Dako). The images were processed with the Image J software developed at the National Institutes of Health (Bethesda, MD, USA). Integrated density was calculated for each image after background subtraction. The background corresponds to the immunoreactivity in the negative control tissue (normal liver). The percentage of the ratio between acetyl histone H3 and histone H3 immunoreactivity was calculated considering 100% the ratio of a positive control tissue (amygdala) added to tissue microarray slides.<sup>24</sup>

### Determination of metabolites and enzymatic activities

Prostaglandin E<sub>2</sub> was determined in culture media by specific immunoassay (Arbor Assays, Ann Arbor, MI, USA).<sup>44</sup> HDAC total activity was analyzed in cell extracts by a fluorimetric detection method (HDAC Assay Kit, Upstate, Billerica, MA, USA).

### Genomic DNA isolation, bisulfite treatment and methylation-specific analysis

Genomic DNAs were isolated from cells or resected specimens using the Maxwell 16 DNA purification Kit (Promega, Madison, WI, USA) and DNA samples were treated with bisulfite using the EZ DNA Methylation-Gold Kit (Zymo Research, Irvine, CA, USA) to convert cytosine to uracil, according to the manufacturer's instructions. A two steps nested-PCR strategy was used to amplify COX-2 CpG islands starting with 1 µl of bisulfate-treated DNA in a final volume of 25 µl. In the first step, a 412-bp fragment was amplified for CpG islands A and B, and a 476-bp fragment for the CpG island C. The PCR cycle used was as follows: 95 °C for 10 min, 40 cycles at 95 °C for 30 s, 58 °C (islands A and B) or 56 °C (island C) for 30 s and 72 °C for 45 s and a final extension at 72 °C for 10 min. A 2.6 µl volume of the first PCR product was used as a template for a new round of amplification in a final volume of 65 µl using a pair of internal primers, one of them a biotin-5'-modified oligonucleotide. A fragment of 368 bp for CpG islands A and B or a 290-bp fragment for CpG island C was amplified using the PCR cycle described above. The final product was purified and pyrosequenced for methylation analysis by the DNA Analysis Facility of the Instituto de Biomedicina de Valencia, Spain. All used primers are detailed in the Supplementary Table 1.

The methylation status was also evaluated by MSRA. After isolation genomic DNA samples were treated with restriction enzymes *MspI* and *HpaII* and amplified by PCR as follows: 95 °C for 10 min and then 30 cycles at 95 °C for 15 s, 58 °C for 30 s and 72 °C for 30 s and a final extension at 72 °C for 7 min. A non-digested sample was used as the positive control. PCR products were visualized on a 2% agarose gels stained with ethidium

bromide. Specific primers used for amplification of each CpG site are shown in the Supplementary Table 2.

### Chromatin immunoprecipitation analysis

Evaluation of histone acetylation levels was performed by chromatin immunoprecipitation analysis as described previously,<sup>45</sup> using isolated nuclei from formaldehyde-cross-linked HuH-6 and HuH-7 cells. Chromatin obtained from untreated (control) or 16 h NaB-treated cells was immunoprecipitated using antibodies against: RNA polymerase II (sc-899, Santa Cruz), Ac-H3 (K9, K14) (06-599, Millipore) and Ac-H4 (K12) (07-595, Millipore). The amount of DNA in each chromatin immunoprecipitated was quantified by real time-PCR on a 7500 Fast System (Life Technologies) using the SYBR Green PCR reagent. The oligonucleotides used for each PCR reaction are listed in the Supplementary Table 3.

### Data analysis

Data are expressed as mean  $\pm$  s.d. (*n* ranged from three to five independent experiments). The Mann-Whitney *U* test was used for ordinal variables. Survival length was determined from the day of primary tumor surgery to the date of death or last clinical follow-up. The Kaplan-Meier method was used for survival analysis grouping with COX-2 methylation or acetylation status. Differences between curves were analyzed using the log-rank test. The statistical software SPSS Statistics 20 (IBM, Armonk, NY, USA) was used; a *P*-value of <0.05 was considered significant.

### CONFLICT OF INTEREST

The authors declare no conflict of interest.

### ACKNOWLEDGEMENTS

We thank Beatriz Agueda, Silvia Aparicio and Benito Alarcón for their technical assistance. This work was supported by the Ministry of Science and Innovation (SAF2010-16037, SAF2009-12602 and BFU2011-24760) and by Comunidad de Madrid (P2010/BMD-2378). CIBERehd is funded by the Instituto de Salud Carlos III. AF-A and NA were supported by the Carlos III Health Institute (Red de Centros FIS-RECAVA RD06/0014/0025).

### REFERENCES

- Simmons DL, Botting RM, Hla T. Cyclooxygenase isozymes: the biology of prostaglandin synthesis and inhibition. *Pharmacol Rev* 2004; **56**: 387–437.
- Ledwith BJ, Pauley CJ, Wagner LK, Rokos CL, Alberts DW, Manam S. Induction of cyclooxygenase-2 expression by peroxisome proliferators and non-tetra-decanoylphorbol 12,13-myristate-type tumor promoters in immortalized mouse liver cells. *J Biol Chem* 1997; **272**: 3707–3714.
- Martin-Sanz P, Callejas NA, Casado M, Diaz-Guerra MJ, Bosca L. Expression of cyclooxygenase-2 in foetal rat hepatocytes stimulated with lipopolysaccharide and pro-inflammatory cytokines. *Br J Pharmacol* 1998; **125**: 1313–1319.
- Casado M, Callejas NA, Rodrigo J, Zhao X, Dey SK, Bosca L *et al*. Contribution of cyclooxygenase 2 to liver regeneration after partial hepatectomy. *FASEB J* 2001; **15**: 2016–2018.
- Rudnick DA, Perlmutter DH, Muglia LJ. Prostaglandins are required for CREB activation and cellular proliferation during liver regeneration. *Proc Natl Acad Sci USA* 2001; **98**: 8885–8890.
- Yamamoto H, Kondo M, Nakamori S, Nagano H, Wakasa K, Sugita Y *et al*. JTE-522, a cyclooxygenase-2 inhibitor, is an effective chemopreventive agent against rat experimental liver fibrosis. *Gastroenterology* 2003; **125**: 556–571.
- Kern MA, Haugg AM, Koch AF, Schilling T, Breuhahn K, Walczak H *et al*. Cyclooxygenase-2 inhibition induces apoptosis signaling via death receptors and mitochondria in hepatocellular carcinoma. *Cancer Res* 2006; **66**: 7059–7066.
- Mayoral R, Fernandez-Martinez A, Bosca L, Martin-Sanz P. Prostaglandin E2 promotes migration and adhesion in hepatocellular carcinoma cells. *Carcinogenesis* 2005; **26**: 753–761.
- Cusimano A, Fodera D, Lampiasi N, Azzolina A, Notarbartolo M, Giannitrapani L *et al*. Prostaglandin E2 receptors and COX enzymes in human hepatocellular carcinoma: role in the regulation of cell growth. *Ann NY Acad Sci* 2009; **1155**: 300–308.
- Cheng AS, Yu J, Lai PB, Chan HL, Sung JJ. COX-2 mediates hepatitis B virus X protein abrogation of p53-induced apoptosis. *Biochem Biophys Res Commun* 2008; **374**: 175–180.
- Nunez O, Fernandez-Martinez A, Majano PL, Apolinario A, Gomez-Gonzalo M, Benedicto I *et al*. Increased intrahepatic cyclooxygenase 2, matrix metalloproteinase 2, and matrix metalloproteinase 9 expression is associated with progressive

- liver disease in chronic hepatitis C virus infection: role of viral core and NSSA proteins. *Gut* 2004; **53**: 1665–1672.
- Cervello M, Fodera D, Florena AM, Soresi M, Tripodo C, D'Alessandro N *et al*. Correlation between expression of cyclooxygenase-2 and the presence of inflammatory cells in human primary hepatocellular carcinoma: possible role in tumor promotion and angiogenesis. *World J Gastroenterol* 2005; **11**: 4638–4643.
- Koga H, Sakisaka S, Ohishi M, Kawaguchi T, Taniguchi E, Sasatomi K *et al*. Expression of cyclooxygenase-2 in human hepatocellular carcinoma: relevance to tumor dedifferentiation. *Hepatology* 1999; **29**: 688–696.
- Kang YJ, Mbonye UR, DeLong CJ, Wada M, Smith WL. Regulation of intracellular cyclooxygenase levels by gene transcription and protein degradation. *Prog Lipid Res* 2007; **46**: 108–125.
- Harper KA, Tyson-Capper AJ. Complexity of COX-2 gene regulation. *Biochem Soc Trans* 2008; **36**(Pt 3): 543–545.
- de Maat MF, van de Velde CJ, Umetani N, de Heer P, Putter H, van Hoesel AQ *et al*. Epigenetic silencing of cyclooxygenase-2 affects clinical outcome in gastric cancer. *J Clin Oncol* 2007; **25**: 4887–4894.
- Murata H, Tsuji S, Tsujii M, Sakaguchi Y, Fu HY, Kawano S *et al*. Promoter hypermethylation silences cyclooxygenase-2 (Cox-2) and regulates growth of human hepatocellular carcinoma cells. *Lab Invest* 2004; **84**: 1050–1059.
- Deng WG, Zhu Y, Wu KK. Role of p300 and PCAF in regulating cyclooxygenase-2 promoter activation by inflammatory mediators. *Blood* 2004; **103**: 2135–2142.
- Coward WR, Watts K, Feghali-Bostwick CA, Knox A, Pang L. Defective histone acetylation is responsible for the diminished expression of cyclooxygenase 2 in idiopathic pulmonary fibrosis. *Mol Cell Biol* 2009; **29**: 4325–4339.
- Yue X, Yang F, Yang Y, Mu Y, Sun W, Li W *et al*. Induction of cyclooxygenase-2 expression by hepatitis B virus depends on demethylation-associated recruitment of transcription factors to the promoter. *Viral J* 2011; **8**: 118.
- Hur K, Song SH, Lee HS, Ho Kim W, Bang YJ, Yang HK. Aberrant methylation of the specific CpG island portion regulates cyclooxygenase-2 gene expression in human gastric carcinomas. *Biochem Biophys Res Commun* 2003; **310**: 844–851.
- Song SH, Jong HS, Choi HH, Inoue H, Tanabe T, Kim NK *et al*. Transcriptional silencing of Cyclooxygenase-2 by hyper-methylation of the 5' CpG island in human gastric carcinoma cells. *Cancer Res* 2001; **61**: 4628–4635.
- Callejas NA, Bosca L, Williams CS, Du BR, Martin-Sanz P. Regulation of cyclooxygenase 2 expression in hepatocytes by CCAAT/enhancer-binding proteins. *Gastroenterology* 2000; **119**: 493–501.
- Uhlen M, Bjorling E, Agaton C, Szigarty CA, Amini B, Andersen E *et al*. A human protein atlas for normal and cancer tissues based on antibody proteomics. *Mol Cell Proteomics* 2005; **4**: 1920–1932.
- Baylin SB, Herman JG, Graff JR, Vertino PM, Issa JP. Alterations in DNA methylation: a fundamental aspect of neoplasia. *Adv Cancer Res* 1998; **72**: 141–196.
- Marks PA, Richon VM, Miller T, Kelly WK. Histone deacetylase inhibitors. *Adv Cancer Res* 2004; **91**: 137–168.
- Giannitrapani L, Ingrao S, Soresi M, Florena AM, La Spada E, Sandonato L *et al*. Cyclooxygenase-2 expression in chronic liver diseases and hepatocellular carcinoma: an immunohistochemical study. *Ann NY Acad Sci* 2009; **1155**: 293–299.
- Esteller M. Cancer epigenomics: DNA methylomes and histone-modification maps. *Nat Rev Genet* 2007; **8**: 286–298.
- Lee S, Lee HJ, Kim JH, Lee HS, Jang JJ, Kang GH. Aberrant CpG island hypermethylation along multistep hepatocarcinogenesis. *Am J Pathol* 2003; **163**: 1371–1378.
- Calvisi DF, Ladu S, Gorden A, Farina M, Conner EA, Lee JS *et al*. Ubiquitous activation of Ras and Jak/Stat pathways in human HCC. *Gastroenterology* 2006; **130**: 1117–1128.
- Calvisi DF, Ladu S, Gorden A, Farina M, Lee JS, Conner EA *et al*. Mechanistic and prognostic significance of aberrant methylation in the molecular pathogenesis of human hepatocellular carcinoma. *J Clin Invest* 2007; **117**: 2713–2722.
- Weisenberger DJ, Siegmund KD, Campan M, Young J, Long TI, Faasse MA *et al*. CpG island methylator phenotype underlies sporadic microsatellite instability and is tightly associated with BRAF mutation in colorectal cancer. *Nat Genet* 2006; **38**: 787–793.
- Yang JD, Seol SY, Leem SH, Kim YH, Sun Z, Lee JS *et al*. Genes associated with recurrence of hepatocellular carcinoma: integrated analysis by gene expression and methylation profiling. *J Korean Med Sci* 2011; **26**: 1428–1438.
- Mossman D, Kim KT, Scott RJ. Demethylation by 5-aza-2'-deoxycytidine in colorectal cancer cells targets genomic DNA whilst promoter CpG island methylation persists. *BMC Cancer* 2010; **10**: 366.
- Xia D, Wang D, Kim SH, Katoh H, Dubois RN. Prostaglandin E(2) promotes intestinal tumor growth via DNA methylation. *Nat Med* 2012; **18**: 224–226.
- Morinaga S, Yamamoto Y, Noguchi Y, Imada T, Rino Y, Akaike M *et al*. Cyclooxygenase-2 mRNA is up-regulated in cirrhotic or chronic hepatitis liver adjacent to hepatocellular carcinoma. *J Gastroenterol Hepatol* 2002; **17**: 1110–1116.
- Um TH, Kim H, Oh BK, Kim MS, Kim KS, Jung G *et al*. Aberrant CpG island hypermethylation in dysplastic nodules and early HCC of hepatitis B virus-related human multistep hepatocarcinogenesis. *J Hepatol* 2011; **54**: 939–947.

- 38 Vidali G, Boffa LC, Bradbury EM, Allfrey VG. Butyrate suppression of histone deacetylation leads to accumulation of multiacetylated forms of histones H3 and H4 and increased DNase I sensitivity of the associated DNA sequences. *Proc Natl Acad Sci USA* 1978; **75**: 2239–2243.
- 39 Tong X, Yin L, Joshi S, Rosenberg DW, Giardina C. Cyclooxygenase-2 regulation in colon cancer cells: modulation of RNA polymerase II elongation by histone deacetylase inhibitors. *J Biol Chem* 2005; **280**: 15503–15509.
- 40 Yamaguchi K, Lantowski A, Dannenberg AJ, Subbaramaiah K. Histone deacetylase inhibitors suppress the induction of c-Jun and its target genes including COX-2. *J Biol Chem* 2005; **280**: 32569–32577.
- 41 Choi YH. Induction of apoptosis by trichostatin A, a histone deacetylase inhibitor, is associated with inhibition of cyclooxygenase-2 activity in human non-small cell lung cancer cells. *Int J Oncol* 2005; **27**: 473–479.
- 42 Liu YW, Wang SA, Hsu TY, Chen TA, Chang WC, Hung JJ. Inhibition of LPS-induced C/EBP delta by trichostatin A has a positive effect on LPS-induced cyclooxygenase 2 expression in RAW264.7 cells. *J Cell Biochem* 2010; **110**: 1430–1438.
- 43 Park GY, Joo M, Pedchenko T, Blackwell TS, Christman JW. Regulation of macrophage cyclooxygenase-2 gene expression by modifications of histone H3. *Am J Physiol Lung Cell Mol Physiol* 2004; **286**: L956–L962.
- 44 Casado M, Molla B, Roy R, Fernandez-Martinez A, Cucarella C, Mayoral R *et al*. Protection against Fas-induced liver apoptosis in transgenic mice expressing cyclooxygenase 2 in hepatocytes. *Hepatology* 2007; **45**: 631–638.
- 45 Fernandez-Alvarez A, Soledad Alvarez M, Cucarella C, Casado M. Characterization of the human insulin-induced gene 2 (INSIG2) promoter: the role of Ets-binding motifs. *J Biol Chem* 2010; **285**: 11765–11774.



*Oncogenesis* is an open-access journal published by Nature Publishing Group. This work is licensed under the Creative Commons Attribution-NonCommercial-No Derivative Works 3.0 Unported License. To view a copy of this license, visit <http://creativecommons.org/licenses/by-nc-nd/3.0/>

Supplementary Information accompanies the paper on the Oncogenesis website (<http://www.nature.com/oncsis>)